Hydrogen tube vehicle for supersonic transport: Analysis of the concept

A. R. Miller[a,*]

[a] *Vehicle Projects LLC and Supersonic Tube Vehicle LLC, 621 17th Street, Suite 2131, Denver, CO 80293, USA*

Abstract

I propose and analyze a concept vehicle that operates in a hydrogen atmosphere contained within a tube, or pipeline, and because of the high speed of sound in hydrogen, it delays the onset of the sound barrier. Mach 1.2 in air corresponds to only Mach 0.32 in hydrogen. The proposed vehicle, a cross between a train and an airplane, is multi-articulated, runs on a guideway, is propelled by propfans, and flies on a hydrogen aerostatic fluid film. Vehicle power is provided by onboard hydrogen-oxygen fuel cells. Hydrogen fuel is taken from the tube itself, liquid oxygen (LOX) is carried onboard, and the product water is collected and stored until the end of a run. Thus, unlike conventional vehicles, it breathes its fuel, stores its oxidant, and its weight increases during operation. Taking hydrogen fuel from the tube solves the problem of vehicular hydrogen-storage, a major challenge of contemporary hydrogen fuel-cell vehicles. The foundation of the feasibility analysis is extrapolation of aerodynamic properties of a mid-sized turboprop airliner, the Bombardier Dash 8 Q400™. Based on the aerodynamic analysis, I estimate that the hydrogen tube vehicle would require 2.0 MW of power to run at 1,500 km/h, which is supersonic with respect to air. It would require 2.64 h to travel from New York City to Los Angeles, consuming 2,330 L of onboard LOX and producing 2,990 L of liquid water during the trip. Part of the feasibility analysis shows that it is possible to package the corresponding fuel-cell stacks, LOX systems, and water holding tanks in the tube vehicle. The greatest technical challenge is levitation by aerostatic hydrogen bearings. Risk of fire or detonation within the tube, similar to that of existing large natural-gas pipelines, is expected to be manageable and acceptable.

Keywords: Aerodynamics; Fuel cells; Gas bearings; Hydrogen; Pipeline; Speed of sound; Supersonic transport

1. Introduction

The speed of commercial aircraft is practically limited by the speed of sound in air, 346 m/s at 298 K, and jet transports typically operate around Mach 0.8. As an airplane enters the transonic region, parts of its surface are subsonic and, because air-stream velocity increases along curvature of its surface, some parts are supersonic. Air becomes strongly compressible near the speed of sound, and the supersonic parts emanate shock waves approximately normal to the surface. The shock waves increase drag (*wave drag*) and decrease lift; as speed of the aircraft varies, movement of the waves on the surface causes buffeting [1,2]. As shown in Figure 1, wave drag gives rise to a power peak at Mach 1 called the "sound barrier."

In this paper, I propose and analyze a concept vehicle that operates in a hydrogen atmosphere contained within a tube, like a large pipeline, and because of the high speed of sound in hydrogen, it delays the onset of the sound barrier. Mach 1.2 in air corresponds to only Mach 0.32 in hydrogen.[1] Thus, the vehicle could reach $M_A = 1.2$, that is, be supersonic with respect to air, while remaining

* Corresponding author. Tel.: + 1 303 296 4218; fax: + 1 303 296 4219.
Email address: arnold.miller@vehicleprojects.com (A.R. Miller)

[1] Mach numbers with respect to the speed of sound in air will be denoted as M_A.

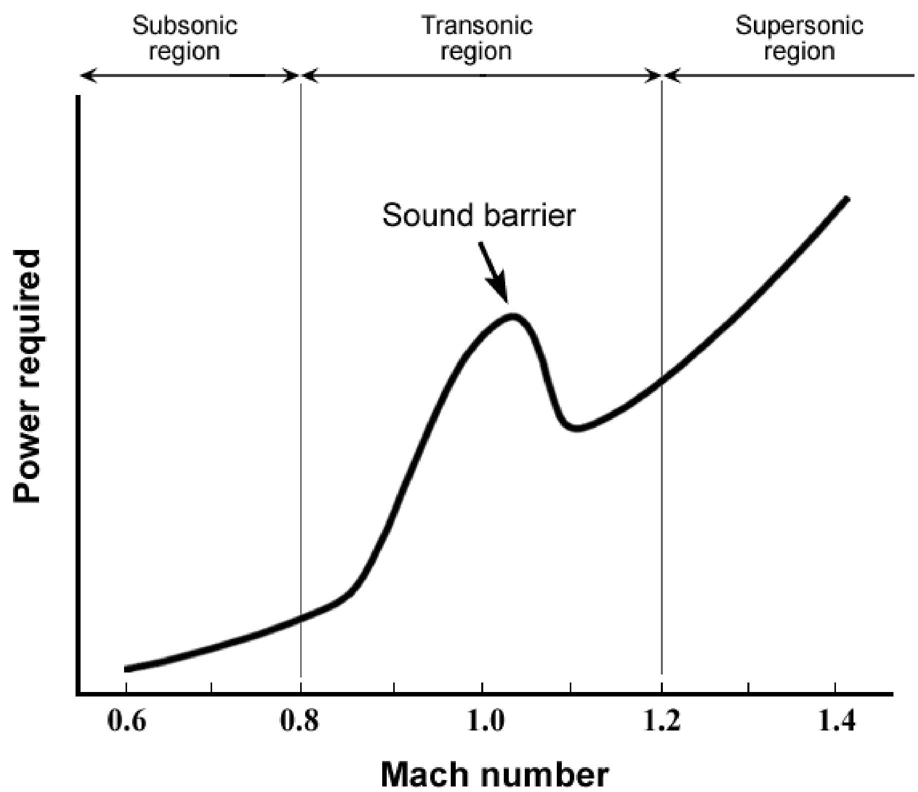

Fig. 1. Aircraft power as a function of Mach number. When the vehicle speed reaches the transonic region, Mach 0.8 – 1.2, propulsion power rapidly rises. The power peak located at Mach 1 is termed the "sound barrier." (Adapted from references [1,2]).

subsonic in the hydrogen atmosphere. As shown in Table 1, a hydrogen atmosphere offers several advantages over air as the operating fluid for a vehicle: high speed of sound results in a high transonic speed, low fluid density ρ gives low pressure drag, low viscosity μ gives low viscous or skin-friction drag, and high thermal conductivity facilitates heat rejection to the operating fluid.

Two somewhat analogous applications exist: (1) Hypersonic rocket sleds reduce drag and aerothermal effects by being rammed at high speed into a disposable polyethylene tunnel inflated with helium [3]. Vehicle drag is an increasing function of fluid density, and the density of helium (0.164 g/L) is only 14% of the density of air [4]. The current world land speed record of 289 thousand m/s (10,400 km/h = 6,450 mi/h) used such a technique. However, because the sled's speed far exceeds the speed of sound in helium (965 m/s), the object of the technique, unlike ours, is not to delay the onset of the sound barrier. (2) Cryogenic hydrogen gas has been proposed as a wind tunnel gas to increase the effective Reynolds numbers of test bodies [5].

The proposed vehicle is a cross between a train and an airplane. It is like a train because it is multi-articulated and runs on a guideway, but it is like an airplane because it is propelled by propfans and flies, or levitates, on a hydrogen aerostatic fluid film. The vehicle operates in a hydrogen-filled tube, like a large pipeline, that is maintained at a pressure slightly above 1 bar absolute. Vehicle power is provided by onboard hydrogen-oxygen fuel cells. Hydrogen fuel is taken from the tube itself, liquid oxygen (LOX) is carried onboard, and the product water is collected and stored until the end of a run.

The vehicle thus gains weight as it operates. Taking hydrogen fuel from the tube solves a major challenge of contemporary hydrogen fuel cell vehicles: storage of hydrogen.

Potential benefits of the proposed transport system include: (1) energy-efficient, supersonic transport from city center to city center with zero emissions and negligible acoustic noise to the environment, (2) operation independent of the weather, (3) low infrastructure cost compared to similarly routed long-stator maglev systems [6], and (4) a solution to the hydrogen storage problem for long-range hydrogen-fueled vehicles. At first thought, hydrogen safety would seem to be an issue, but I will argue below that system risk is similar to that of a natural-gas pipeline and can be satisfactorily

managed. The principal challenges facing the system are: (1) high absolute infrastructure cost, (2) maintenance of adequate hydrogen gaps in the aerostatic levitation and guidance system, and (3) possibly dynamic instability of the levitated vehicle.

Table 1
Properties[1] of Hydrogen versus Air

Properties	Hydrogen	Air	Hydrogen Value/Air Value
Speed of Sound, m/s (km/h)	1,310 (4,720)	346 (1,246)	3.8
Density (ρ), g/L	0.082	1.16	0.071
Viscosity (μ), μPa-s	9.0	18.6	0.48
Thermal Conductivity, mW/m-K	187	26.2	7.1

[1] At pressure P = 1 bar and temperature T = 298-300 K [4]

This paper analyzes the feasibility of the concept of a hydrogen tube vehicle for supersonic transport. It proposes a conceptual design – power source, propulsion, levitation, and guidance – and then analyzes its feasibility – power and energy requirements, vehicle packaging, levitation by gas bearings, and safety. Substantial future progress will require experimental studies of the fluid-film levitation and guidance system, hydrogen wind-tunnel tests of vehicle-in-tube aerodynamics, and the development and demonstration of proof-of-concept prototypes.

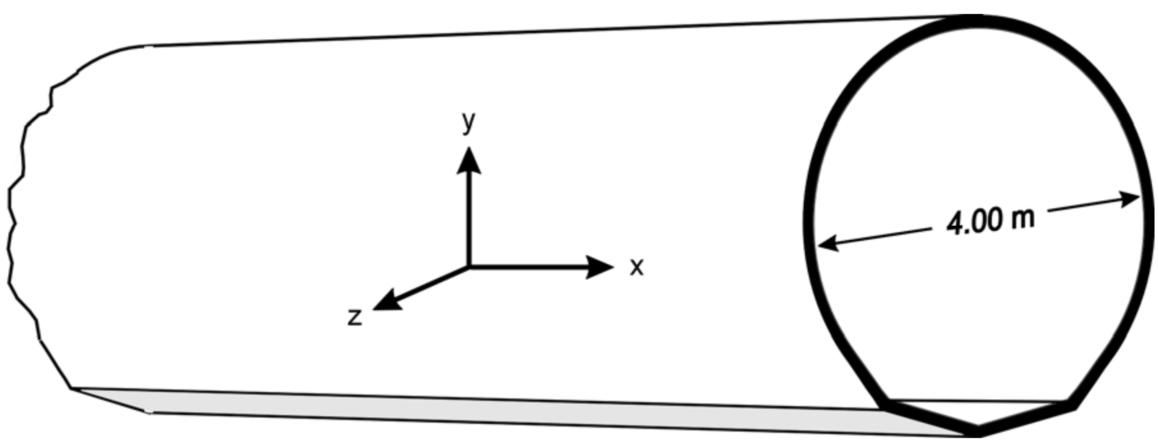

Fig. 2. Schematic of the hydrogen tube. The vee-way, the levitation and guidance rail, is shown at the bottom of the 4.00-m inside-diameter tube. The x-axis of the modified right-handed coordinate system is the center of the tube, which may curve in three-dimensional space. The y-axis is orthogonal to the x-axis and bisects the symmetrical vee-way. The z-axis is orthogonal to both x- and y-axes.

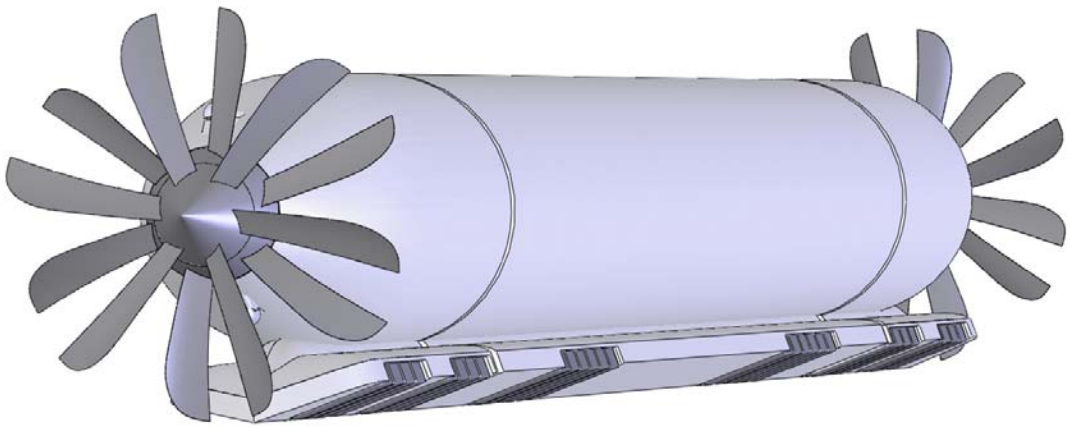

Fig. 3. Three-dimensional computer model of hydrogen tube vehicle. This depiction consists of one passenger car and the usual two locomotives, one at each end. Additional details of the locomotives are provided in Figures 4 and 5, and details of the car, based on the Bombardier Dash 8 Q400 propjet airliner, are given in the "Feasibility" section. Multiple passenger or freight cars could be employed between the same two locomotives. The locomotive trucks, aerostatic gas bearing pads, have four segments each, whereas the car trucks have six segments.

2. Concept

The tube, or pipeline, in which the vehicle operates will be maintained at a hydrogen pressure slightly above atmospheric so that any leakage will be to the outside of the tube. At the bottom of the tube is a V-shaped section, the *vee-way*, that is the levitation and guidance rail for the aerostatic gas bearings (see Figure 2). A 4.00-m inside diameter is arbitrarily chosen so that the tube will accommodate a vehicle of 2.69-m outside diameter, the fuselage diameter of the Bombardier Dash 8 Q400™, a midsized turboprop airliner whose aerodynamic analysis is the basis for the feasibility analysis. A diameter of 4.00 m is not unusually large for a pipeline: the Great Man-Made River water project in Libya includes 380 km of 4-m concrete pipe [7] and the first Los Angeles Aqueduct, since 1913, includes steel-pipe sections of 8-12 ft diameter [8]. Pipeline engineering is a well-established discipline, and large pipelines carry crude oil, natural gas, water, waste water, slurries, and pneumatic capsules throughout the world [9,10]. They are laid aboveground, underground, and submarine. Our hydrogen tube will follow standard engineering practice for routing, but unlike most pipelines, the hydrogen tube must have large-radius curves to maximize clearances within the gas-bearing levitation system (see below). The tube will require a support infrastructure: (1) makeup hydrogen must be supplied to replace that consumed by the vehicle, (2) airlocks should be located at intervals along the tube to allow rescue of a disabled vehicle, and (3) air and water vapor inevitably introduced as impurities must be removed. Aside from the hydrogen purification system, however, the infrastructure cost is expected to be similar to a water pipeline and less than a long-stator maglev system [6].

To minimize infrastructure cost per kilogram-kilometer of payload and improve high-speed aerodynamics, the proposed vehicle is long and slender. Similar to a train, it is multi-articulated and consists of cars and locomotives, one at each end. Multiple articulation joints along the x-axis (Fig. 2) allow it to conform to curvature of the tube in three-dimensional space. Figures 3 and 4 show a computer model of the vehicle, consisting of one passenger car and the two locomotives; Figure 5 is a scale drawing of one of the locomotives in the tube. Details of the passenger car are discussed below in the "Feasibility" section. Like the locomotives, the car has two sets of bearing pads, which are homologous to the trucks (bogies) of a conventional rail vehicle.

Propulsion is via propfans, high-solidity propellers, on each locomotive. Propfans [11-12], especially contra-rotating versions, approach 90% efficiency in practice. Propeller efficiency is defined as

$$\eta = \frac{TV}{p_s} \quad (1)$$

where T is thrust, V is velocity of the vehicle, and p_s is shaft input mechanical power. The Froude momentum theory of propulsion [13] provides understanding of the factors affecting efficiency: Assume the operating fluid (gas) is accelerated by an infinitely thin "actuator disc" of area S that provides energy to the gas but offers no resistance to gas passing through it. In unit time, the mass of fluid passing through the actuator disc is

$$m = \rho S V_0 \quad (2)$$

where ρ is density of the gas and V_0 is the gas velocity at the immediate rear of the disc. The increase of momentum of this mass of fluid, and hence the thrust T on the disc, is

$$\Delta(\mathrm{mv}) = T = \rho S V_0 \left(V_s - V\right) \quad (3)$$

where V is the gas velocity far ahead of the disc and V_s is the gas velocity far behind the disc.

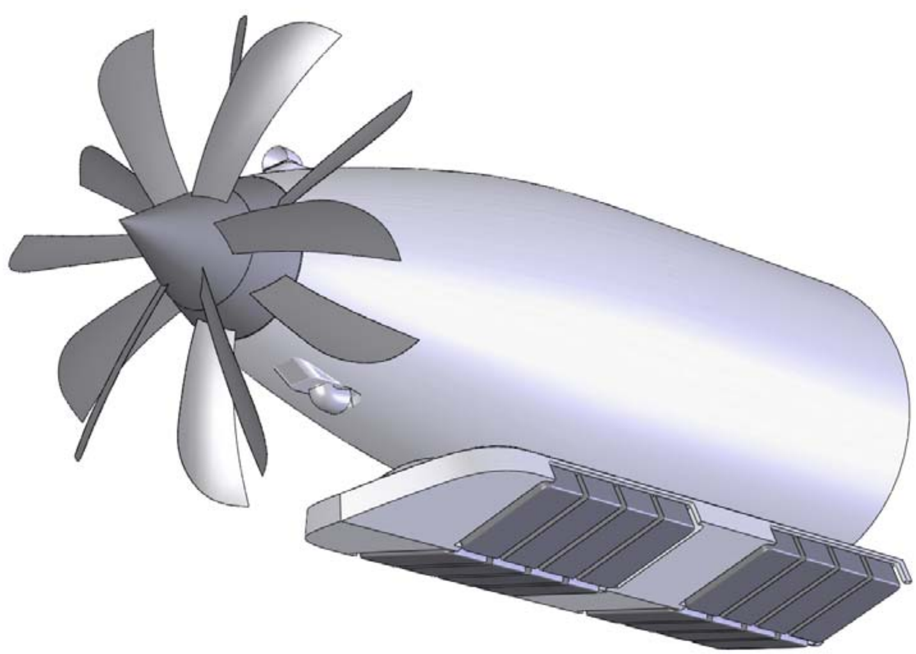

Fig. 4. Detail of locomotive. The model shows the contra-rotating propfan and four-segment gas-bearing pads. Each group of four segments, whose gas pressure and geometry can be independently and actively varied, constitutes a *bearing pad* and corresponds to a truck (bogie) of a conventional rail vehicle.

Following a number of steps [13], it can be shown that the ideal efficiency of the actuator disc is

$$\eta_i = \frac{2}{1 + \frac{V_s}{V}} \tag{4}$$

The closer a propeller approximates the assumptions of an ideal actuator disc, the better the theory applies and the higher the actual efficiency [11]: more blades, wider blades, and uniform distribution of thrust on the blades all lead to higher efficiency. Propeller tip speed is greater than vehicle speed because a component of rotational velocity adds to vehicle translational velocity, and tip speed entering the transonic region limits the speed of conventional propeller aircraft. Propfans allow higher aircraft speed by using blades having the swept-back shape of a supersonic airfoil; contra-rotating propfans furthermore avoid energy loss to rotation of the slipstream. For example, the 41-MW, 130-tonne turbo-propfan Antonov An-70 can operate at near-jet speeds with a claimed propeller efficiency of 90%, substantially higher than the most efficient fanjets [14,15]. From equation (4), efficiency increases toward unity as $V_s \rightarrow V$. Thus, as per Equation (3), a propeller should have the largest possible diameter (large S) to obtain the needed thrust while minimizing ($V_s – V$). To avoid supersonic speed of the propeller tips, a propeller with large S should be slow-turning. It is noteworthy that the final equation for efficiency, Equation (4), is independent of gas density ρ.

The principal benefits of propellers for propulsion in the tube, in particular contra-rotating propfans, are (1) zero infrastructure cost, (2) high efficiency, as discussed above, and (3) zero net torque acting on the vehicle. Compared to single-rotating propellers, however, contra-rotating propellers are costlier, heavier, and noisier. The noise problem is being addressed in ongoing work, including active noise cancellation techniques [12], and the Bombardier Q400, though using only single-rotating propellers, uses noise cancellation technology [16].

Primary braking of the tube vehicle will be achieved by increasing the pitch of the propeller blades beyond the feathered position, a standard method of braking an aircraft upon landing [2].

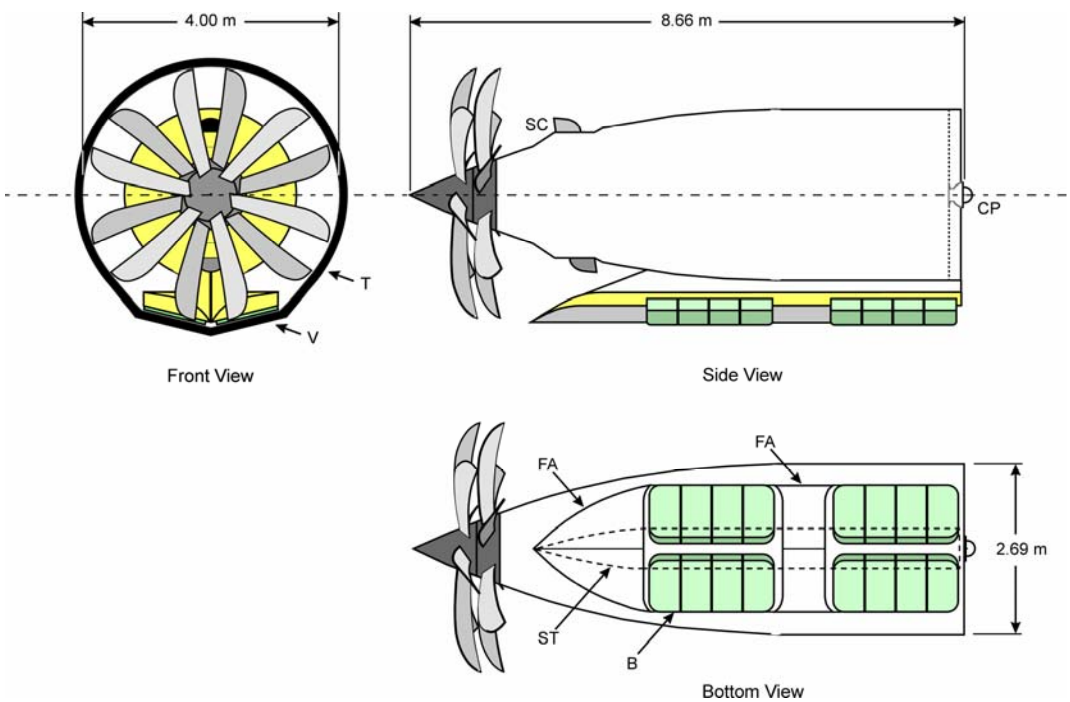

Fig. 5. Scale drawing of locomotive in the hydrogen tube. T = hydrogen tube, V = vee-way, SC = hydrogen scoop; CP = genderless ball-and-socket coupling, FA = fairing for streamlining the bearing-pad unit, ST = strut supporting fuselage above gas-bearing unit, B = four-segment gas-bearing pad conforming to vee-way.

Reversal of the vehicle will involve rotation of the blades by 180^o around their radial axes, followed by reversal of rotational direction of the propellers.

The tube vehicle breathes fuel from the hydrogen atmosphere and stores its oxidant onboard. In the opposite manner to conventional hydrogen-air fuel cells, hydrogen flows through the stacks and the oxygen, from onboard LOX, is dead-ended. Because release of water vapor to the tube atmosphere is to be avoided, a fuel cell producing water at the cathode is desirable. Thus, the fuel cell should use an acid electrolyte, and the proton-exchange membrane (PEM) type is attractive because of its high power density. Hydrogen PEM fuel cells operating on oxygen additionally have 30% higher power density than when operating on air [17]. Liquid water will be purged from the cathode chamber and stored in a holding tank until the vehicle completes a run. Because of the very high thermal conductivity of hydrogen (Table 1), I propose that the liquid-to-hydrogen heat exchanger for the powerplant can employ only the smooth surface of each locomotive.

For a high-speed vehicle operating in an enclosed, clean gas, a gas bearing is an attractive levitation method. Gas bearings may be either *self-acting* (or *hydrodynamic*), in which case the fluid film is generated by the motion of the bearing pad itself, or *externally pressurized* (*hydrostatic or aerostatic)*, in which case the bearing film is provided externally by a gas pump. Both types offer the advantages of near-zero running friction, no wear, high stiffness, and no environmental contamination by the lubricating fluid; aerostatic bearings additionally offer zero static friction [18,19]. With the exception of aerostatic bearings with compliant seals, both types of gas bearings require high mechanical accuracy and structural stability.

Self-acting gas bearings are used to support the flying heads of computer disc drives [20] and to levitate hypersonic rocket sleds [3,21]. Disadvantages of self-acting bearings include: (1) The fluid-film gap h is an increasing function of pad speed, and hence the bearing provides no support at zero speed. (2) At any speed, the gap is small and h = 2.5 μm is not uncommon [20].

In contrast, externally pressurized, or aerostatic, gas bearings are supported on a gas film generated by an external pump; under constant load, gas pressure, and gas flow, they operate at nearly constant gap h at all speeds. When they use compliant seals, the gap can be larger than for self-acting gas bearings. Figure 6 shows a commercial application of externally pressurized air bearings to move a locomotive across a concrete factory floor during manufacture. The locomotive, weighing 136 t, is supported by two air-bearing pads, one fore and one aft [22]. Operation on the relatively inaccurate surface of a concrete floor is possible by using a compliant

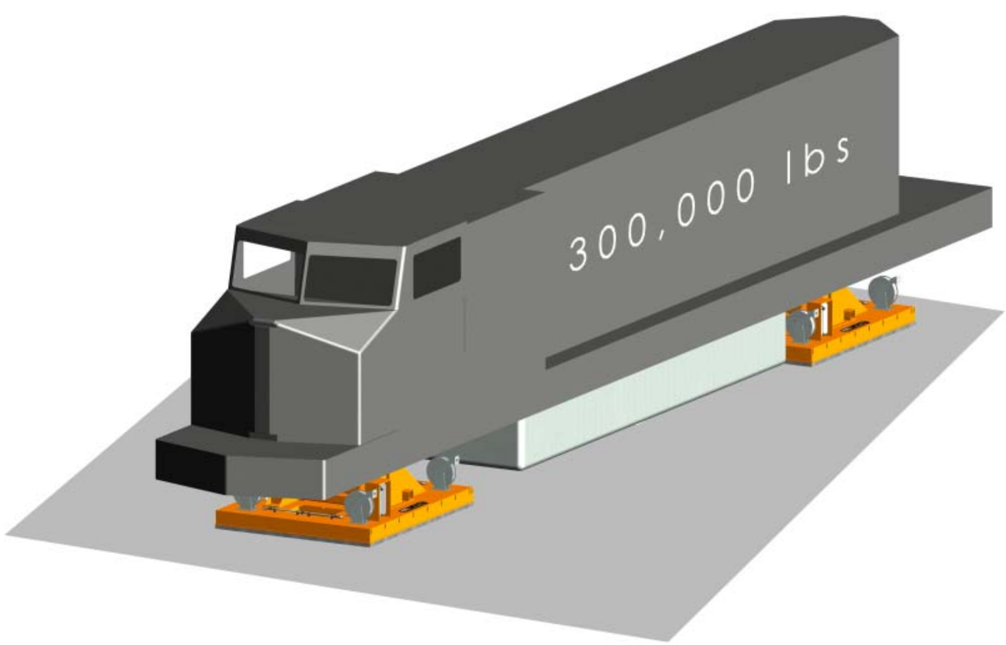

Fig. 6. Commercial application of aerostatic air bearings. Externally pressurized air bearings support this locomotive while it is moved across a factory floor during manufacture. The bearings use compliant gas seals. (Illustration, except for the underlying plane, courtesy of Airflow, LLC)

urethane seal surrounding the pad. The air pump to levitate the load provides a flow of 240 SCFM at a pressure of 60 psi gauge [23] (i.e., 0.113 m^3/s at 414 x 10^3 N/m^2), which corresponds to a power of 47 kW. The larger the gap, however, the more difficult is maintenance of dynamic stability through squeezed-film damping, which decreases as a function of the third power of gap height *h* [24]. Although externally pressurized bearings can support the load at zero speed, the literature states that they would still require a support structure when the vehicle is turned off because they are not able to exert lift when *h* = 0 [21]. However, our experience (see Appendix) shows that they can be self-lifting.

Table 2
Comparison of Airliner and Tube Vehicle

Parameter	**Bombardier Dash 8 Q400** [1]	**Tube Vehicle (Conceptual Design)**
Number of occupants	78 (74 pass. + 4 crew)	76 (74 pass. + 2 crew)
Fuselage maximum diameter, m	2.69	2.69
Cabin maximum internal width, m	2.51	2.51
Baggage volume aft [2], m^3	11.6	11.6
Cabin plus aft baggage-hold length,[3] m	22.5	21.30
Total vehicle length, m	32.84	39.17 (train of Fig 3)
Tube inside diameter, m	Not applicable	4.00
Propeller diameter, m	4.11	3.95
Number of propellers (blades each)	2 (6 ea.)	4 (6 ea.)
Propeller type	Single-rotating	Contra-rotating pairs
Max cruise speed, km/h (Mach number)	667 (M_A = 0.54) [4]	1,500 (M_A = 1.2) [5]
Maximum operating altitude, m	7,620	~ 0
Cruise power, MW	5.9 (2 x 2.94)	2.0 (2 x 1.0) (computed)
Energy consumption [6], MJ	36 x 10^4	3.8 x 10^4

[1] Data from reference [16] unless otherwise noted [2] Reference [15] [3] Measured from floor plan [15]; excludes flight deck but includes aft baggage hold [4] 185 m/s [5] 415 m/s [6] Note added in proof: Using the same method described in the text for the supersonic tube vehicle, but assuming a thermodynamic efficiency of 0.35 for the gas-turbine powerplant, the energy consumption of the Q400 to travel from New York City to Los Angeles is computed as 36 x 10^4 MJ. Because the range of the Q400 is only 2,522 km, the trip would require refueling en route.

For the hydrogen tube vehicle, I propose externally pressurized gas bearings operating on hydrogen supplied from the tube atmosphere by an onboard pump. As illustrated in Figures 2 and 5, the bearing pads conform to the vee-way in the bottom of the hydrogen tube and the pads are segmented – the geometry of the segments (four segments in each locomotive truck) can be varied independently by servomechanisms. Vee-ways are standard elements of machine design and have been used in robust air-bearing systems [24]. Bearing pads comprised of porous graphite, for example, are a commercialized method of gas delivery to the gap [19]. The self-acting effect of pad speed is considered incompatible with externally pressurized levitation [21].

The greatest challenges to development of externally pressurized gas bearings for the high-speed hydrogen tube vehicle are maintenance of adequate hydrogen gap between pads and vee-way and possibly the dynamic stability of the levitated vehicle, although not enough is known about its stability to make a definitive statement. If the gap is too small, the bearing pads may drag on the vee-way, and if too large, the stiffness and dynamic stability decrease. The bearing pads must conform to a curved vee-way when the tube curves in three-dimensional space and to a twisted vee-way when the xy-plane tilts in a curve. I propose a dynamically controlled bearing pad geometry, which has been proposed and tested for machine tools (for a brief review, see reference [24]). For the tube vehicle, sensors would determine the vee-way geometry ahead of the vehicle and servomechanisms would adjust the pad geometry to the vee-way by tilting or rotating the pad segments with respect to the y-axis, adjusting the included angle between the pad segments, and varying the hydrogen pressure to the individual pad segments. With reference to automotive *active suspension systems*, we will refer to this system as an "active levitation system." The active levitation system to control gap height and vehicle stability is analogous to the dynamically controlled electromagnetic suspension (EMS) of maglev trains [6,25]. Preloading the gas-bearing pad, either magnetically or by vacuum, is a common method for maintaining dynamic stability of externally pressurized bearings. If preloading or other external stabilization is necessary for the tube vehicle, airfoils may be effective.

3. Feasibility

To analyze the feasibility of the proposed hydrogen tube vehicle, I will compare its most salient features to known parameters of a mid-sized turboprop airliner, the Bombardier Dash 8 Q400 (see Figure 7). Table 2 displays several parameters of the Q400 and corresponding values either set or calculated for the hydrogen tube vehicle. Figure 8 shows the layout of a hydrogen-tube passenger car; the diagram is based on the floor plan for the Q400 [15] but with the flight deck removed and the rear baggage compartment converted to a cylinder.

To estimate the power required to propel the tube vehicle at 415 m/s ($M_A = 1.2$), we will first compute the change in drag and power if we increased the speed of the Q400 airplane from 185 m/s ($M_A = 0.54$) to 415 m/s and simultaneously changed the atmosphere from air at 7,620-m altitude to hydrogen at 1 bar. As a key to the notation below, subscripts "1" and "2" refer respectively to the two sets of conditions just described:

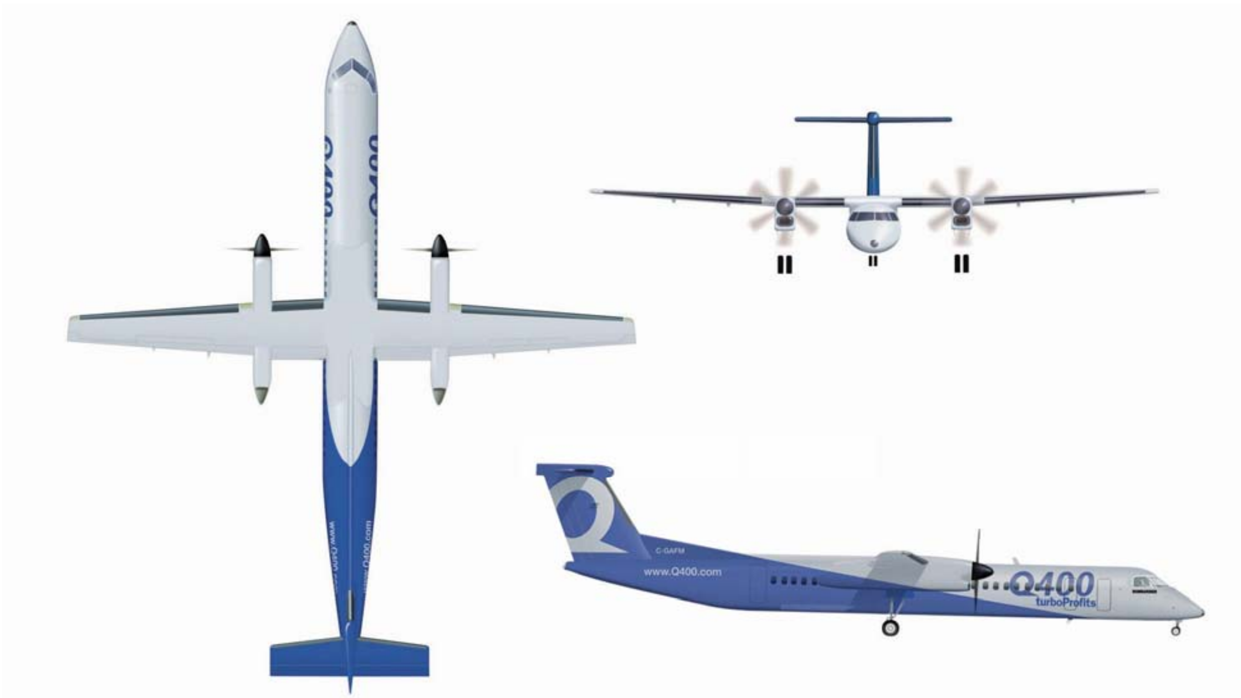

Fig. 7. Bombardier Dash 8 Q400. Specifications of this mid-sized turboprop airliner are given in Table 2. The feasibility analysis compares the hydrogen tube vehicle with this airplane. (Courtesy of Bombardier Aerospace [16])

Condition 1: The Q400 at 185 m/s in air at 7,620-m altitude
Condition 2: The Q400 at 415 m/s in hydrogen at 1 bar pressure

At subsonic speeds, the total drag D_t on an airplane is given by [1,26]

$$D_t = D_p + D_i \qquad (5)$$

where D_p is parasitic drag, which is the sum of pressure drag and viscous (or skin-friction) drag, and D_i is induced drag, the drag caused by diverting the incoming air stream to downwash by the wings. Parasitic drag is given by the equation

$$D_p = 1/2\, C_p A \rho V^2 \qquad (6)$$

where C_p is the parasitic-drag coefficient, A is the frontal (or other) area of the vehicle, ρ is the fluid

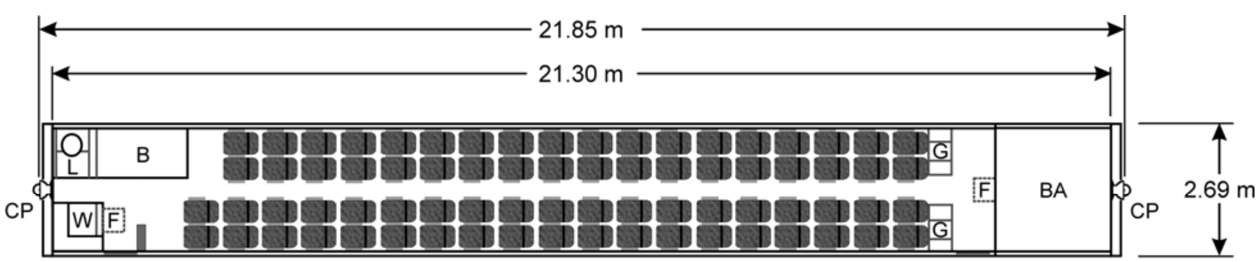

Fig. 8. Layout of a passenger car. This is the middle segment, a 74-passenger car, of the vehicle shown in Fig. 3. Design is based on the Bombardier Dash 8 Q400 airliner, with flight deck removed and the aft baggage compartment replaced by an equal-volume cylinder. L = lavatory, B = front baggage hold, W = wardrobe, F = folding crew seat, D = passenger door, G = galley, S = service door, BA = aft baggage hold, CP = genderless ball-and-socket coupling. (Drawing derived from Q400 cabin layout of reference [15])

density, and V is velocity. Induced drag is given by

$$D_i = \frac{C_i W^2}{1/2\, b^2 \rho V^2} \tag{7}$$

where C_i is the induced-drag coefficient, which depends primarily on the shape and angle of attack of the airfoil, W is aircraft weight, and b is the wing span.

Let D_{p1} and D_{i1} be, respectively, the parasitic and induced drag on the Q400 under Condition 1: velocity $V_1 = 185$ m/s in air at an altitude of 7,620 m, which corresponds to a density of $\rho_1 = 0.56$ kg/m^3 [4]. Let D_{p2} and D_{i2} be, respectively, the parasitic and induced drag on the same aircraft under Condition 2: velocity $V_2 = 415$ m/s in hydrogen at a pressure of 1 bar, which has a density of $\rho_2 = 0.082$ kg/m^3 (Table 1). Therefore, the ratio of parasitic drags in going from Condition 1 to Condition 2 is

$$\frac{D_{p2}}{D_{p1}} = \frac{1/2\, C_p A \rho_2 V_2^2}{1/2\, C_p A \rho_1 V_1^2} \tag{8}$$

$$= \frac{1/2\, C_p A \left(0.082\ \text{kg/m}^3\right)(415\ \text{m/s})^2}{1/2\, C_p A \left(0.56\ \text{kg/m}^3\right)(185\ \text{m/s})^2} \tag{9}$$

$$= 0.737 \tag{10}$$

Similarly, for the ratio of induced drags, we have

$$\frac{D_{i2}}{D_{i1}} = \frac{\dfrac{C_i W^2}{\frac{1}{2} b^2 \rho_2 V_2^2}}{\dfrac{C_i W^2}{\frac{1}{2} b^2 \rho_1 V_1^2}} \tag{11}$$

$$= \frac{\dfrac{C_i W^2}{1/2\, b^2 \left(0.082\ \text{kg/m}^3\right)(415\ \text{m/s})^2}}{\dfrac{C_i W^2}{1/2\, b^2 \left(0.56\ \text{kg/m}^3\right)(185\ \text{m/s})^2}} \tag{12}$$

$$= 1.36 \tag{13}$$

Thus, the parasitic drag is actually decreased, even though the velocity is more than doubled, if the atmosphere is changed to hydrogen. The induced drag, however, is increased. The increase in induced drag with low fluid density is consistent with the observation that induced drag of airplanes increases as a function of altitude [26]. An implication of this is that hydrogen is not an attractive atmosphere for aircraft, at least, for producing lift. A fundamental difference between the lift created by an airfoil and the lift by a gas bearing, proposed here, is that the former is based on gas density ρ, whereas the latter is based on gas viscosity μ (see p. 45 of reference[18]). Because the density of hydrogen is only 7% that of air (see Table 1) but its viscosity is 48%, hydrogen aerostatic bearings should work much better than hydrogen wings. Separate from levitation, Equation (4) indicates that propeller efficiency is independent of fluid density ρ and thus propulsion by propellers in a hydrogen atmosphere should work fine.

We observe from Equations (8) and (11) that

$$\frac{D_{p2}}{D_{p1}} = \frac{D_{i1}}{D_{i2}} \tag{14}$$

which is consistent with our calculation.

Because an airplane is in equilibrium at a fixed velocity and therefore thrust $T = D_t$, power p is given by

$$p = TV = D_t V = \left(D_p + D_i\right) V \tag{15}$$

and thus, from Equations (6) and (7), power to overcome parasitic drag *increases* as a function of the third power of velocity but power to overcome induced drag *decreases* as a function of the first power of V. We can now compute the change in power, as a ratio, if we take the Q400 from Condition 1 to Condition 2. Let p_1 be the power required by the Q400 at the first set of conditions, and let p_2 be the power at the second set of conditions. Hence

$$p_2 = p_1 \frac{\left(D_{p2} + D_{i2}\right) V_2}{\left(D_{p1} + D_{i1}\right) V_1} \tag{16}$$

From our results in Equations (10) and (13), we can write the numerator of Equation (16) in terms D_{p1} and D_{i1}, which gives

$$p_2 = p_1 \frac{\left(0.737\, D_{p1} + 1.36\, D_{i1}\right) V_2}{\left(D_{p1} + D_{i1}\right) V_1} \tag{17}$$

If we make the reasonable assumption that the Q400 is minimized for drag at its cruise speed, then [26]

$$D_{p1} = D_{i1} \tag{18}$$

and Equation (17) reduces to

$$p_2 = p_1 \frac{\left(0.737\, D_{p1} + 1.36\, D_{p1}\right) V_2}{2\, D_{p1} V_1} \tag{19}$$

$$p_2 = 1.05\, p_1 \frac{V_2}{V_1} \tag{20}$$

and from Table 2

$$p_2 = 1.05\,(5.9\ \mathrm{MW}) \frac{415\ \mathrm{m/s}}{185\ \mathrm{m/s}} \tag{21}$$

$$p_2 = 14\ \mathrm{MW} \tag{22}$$

which is my estimate of the power required by the Q400 to fly at 415 m/s in a hydrogen atmosphere.

This power estimate of 14 MW is too high for the tube vehicle operating at 415 m/s ($M_A = 1.2$) in the hydrogen tube for two reasons: (1) The tube vehicle is wingless and tailless and will have a lower parasitic drag than the Q400 at any speed or in any atmosphere. (2) Because it does not receive lift from wings, the tube vehicle has no induced drag. Although the tube vehicle requires some power for levitation, much less power is required to levitate a vehicle by gas bearings at less than 1 mm than fly it on wings at 7,620 m.

The distinction between parasitic and induced drag of an aircraft's wings should be emphasized: The parasitic drag is caused by the differential air pressure on the frontal area of the wing, as well as the skin-friction of the wing surface. In contrast, induced drag is caused by the force on the wing needed to deflect the incoming air to downwash and thereby create lift. If a wing has zero lift (by having a zero effective angle of attack [1]), it will have no induced drag but will still suffer parasitic drag.

We will proceed first by finding the fraction of the total drag D_{t2} of the Q400 under Condition 2 that is due to parasitic drag D_{p2}. Because the induced drag is zero for the tube vehicle, we would then have an upper bound on its total drag as D_{p2}. The desired fraction is

$$\frac{D_{p2}}{D_{t2}} = \frac{D_{p2}}{D_{p2} + D_{i2}} \tag{23}$$

Dividing both numerator and denominator of the right-hand side by D_{p1} gives

$$\frac{D_{p2}}{D_{t2}} = \frac{\frac{D_{p2}}{D_{p1}}}{\frac{D_{p2}}{D_{p1}} + \frac{D_{i2}}{D_{p1}}} \quad (24)$$

By the assumption made before – that the Q400 is minimized for drag at its designed cruise speed, Condition 1, and hence its parasitic and induced drags are equal [26] – Equation (18) allows the following variation of Equation (24):

$$\frac{D_{p2}}{D_{t2}} = \frac{\frac{D_{p2}}{D_{p1}}}{\frac{D_{p2}}{D_{p1}} + \frac{D_{i2}}{D_{i1}}} \quad (25)$$

All of the fractions on the right-hand side are assigned numerical values by Equations (10) and (13), and hence

$$\frac{D_{p2}}{D_{t2}} = \frac{0.737}{0.737 + 1.36} = 0.35 \quad (26)$$

It similarly follows that

$$\frac{D_{i2}}{D_{t2}} = 0.65 \quad (27)$$

The power p_2 required by the Q400 to fly at a velocity of V_2 = 415 m/s in hydrogen (namely, 14 MW by my calculation above) is given by

$$p_2 = D_{t2} V_2 = D_{p2} V_2 + D_{i2} V_2 \quad (28)$$

But for the tube vehicle, the induced drag is zero and hence the power component of the Q400 to overcome parasitic drag only is

$$p_{p2} = D_{p2} V_2 \quad (29)$$

From Equation (26), we have

$$p_{p2} = D_{p2} V_2 = 0.35\, D_{t2} V_2 \quad (30)$$

$$= 0.35\, p_2 = 4.9 \text{ MW} \quad (31)$$

Comparing this result with the total power of the Q400 to fly under Condition 2, given by Equation (22) as 14 MW, illustrates the large price, as the energy and power to overcome induced drag, that aircraft pay to fly above the weather, and the high cost of induced drag is the primary reason that aircraft require as much as 50 times more energy per kilogram-kilometer of payload than rail [27].

This value of the power component p_{p2}, the power to overcome only parasitic drag in the aircraft, is still too high for the total power of the hydrogen tube vehicle. It is too high because it includes the parasitic drag of fuselage, wings, tail, and engine nacelles, whereas the tube vehicle has no wings, tail, or engine nacelles. On the other hand, the tube vehicle does have bearing pads and fairing, which cause parasitic drag.

Approximating the tube vehicle by the Q400 fuselage, we will estimate the fraction of the parasitic drag of the Q400 due only to the fuselage as the ratio of frontal areas. From Equation (6) for parasitic drag, if bodies have similar shapes and hence similar parasitic drag coefficients, the drag will increase directly with frontal area A; all of the components of aircraft approximate the standard airfoil shape. We will thus assume that D_{pf}, the parasitic drag for the fuselage as a hypothetical separate body, and D_{pt}, the parasitic drag for the complete Q400, are approximated as follows:

$$\frac{D_{pf}}{D_{pt}} \cong \frac{A_f}{A_t} \qquad (32)$$

where A_f is the frontal area of the fuselage and A_t is the frontal area of the complete airplane. From measurement of an expanded line drawing [15] of the front view of the Q400 shown in Figure 7, I estimate that

$$\frac{A_f}{A_t} = 0.23 \qquad (33)$$

Hence, the power p_{pf} to propel the Q400 fuselage alone at Condition 2 is derived as follows. From Equation (32)

$$D_{pf} \cong D_{pt}\left(\frac{A_f}{A_t}\right) \qquad (34)$$

$$p_{pf} \cong D_{pf} V_2 = D_{pt} V_2 \left(\frac{A_f}{A_t}\right) = p_{p2}\left(\frac{A_f}{A_t}\right) \qquad (35)$$

$$\cong 0.23\,(4.9\ \mathrm{MW}) = 1.1\ \mathrm{MW} \qquad (36)$$

Although the fuselage of the tube vehicle will have similar drag to the fuselage of the Q400, the value of power given in Equation (36) is too small for the tube vehicle as a whole. Besides fuselage parasitic drag, the tube vehicle also suffers drag from its bearing-pad structure and requires power to operate the bearing hydrogen pump. (Moreover, a new source of parasitic drag, viscous drag with the inner tube surface, may be introduced in the enclosed tube versus a free hydrogen atmosphere.) Thus, Equations (31) and (36) establish error bounds for the true value of power, p_H, required by the tube vehicle to operate at M_A = 1.2 in a free hydrogen atmosphere at 1 bar:

$$1.1\,\mathrm{MW} \le p_H \le 4.9\,\mathrm{MW} \tag{37}$$

Although the power requirements of the bearing parasitic drag, levitation power, and possibly viscous drag with the tube are unknown, I believe they collectively will be less than 1 MW. Hence my estimate for the total continuous propulsion power p_H for the tube vehicle operating at 415 m/s in the hydrogen tube is:

$$p_H \cong 2.0\,\mathrm{MW} \tag{38}$$

The most basic question concerning feasibility of the supersonic tube vehicle is whether the hydrogen-oxygen fuel cells, LOX oxidant, and water holding tank can be packaged onboard. If they cannot be packaged for operation of the vehicle at supersonic speeds over practical distances, the vehicle is not feasible. The fuel cells, LOX, and water will be distributed equally between the two locomotives of the articulated vehicle.

State-of-the-art prototype hydrogen-air PEM fuel-cell stacks have continuous (gross) power densities of around 2.0 kW/L. Operation on oxygen, rather than air, further increases power density by 30% [17], and thus a reasonable volumetric gross power density is 2.6 kW/L. Net power is reduced by parasitic losses in the balance of plant, and the largest of these is due to the air system. Based on our experience in developing large fuel-cell vehicles such as locomotives [28], the efficiency of the balance of plant (net power divided by gross power) of a conventional powerplant would increase from about 0.75 to 0.90 if there were no parasitic losses due to the air system. Because the hydrogen tube vehicle has no air system and moreover because the hydrogen passively flows through the stacks, I will assume the efficiency of the balance of plant is 0.90. Because each locomotive requires 1.0 MW of continuous net power, we therefore need 1.1 MW gross power for each. This requires a stack volume of 423 L, or 0.42 m^3, and corresponds to the volume of a cube with 0.75-m sides.

From the hydrogen tube vehicle's net cruise power, efficiency, cruise speed, and the distance traveled on a practical run, we can compute its stored energy requirement and the volume of onboard LOX. Assume the supersonic tube vehicle operates nonstop between New York City and Los Angeles, a great-circle distance of 3,960 km. Ignoring the time for acceleration, the vehicle operating at its cruise speed of 1,500 km/h will require 2.64-h transit time. A continuous net power of 2.0 MW is required to maintain this speed. We will conservatively assume that the fuel-cell powerplant has an overall thermodynamic efficiency (electrical energy divided by chemical energy) of 0.50. The total power consumption by the vehicle is therefore 4.0 MW, with 2.0 MW being net electrical output and 2.0 MW being thermal output (which includes the losses discussed above in the balance of plant). Accordingly, the energy required for the trip is 3.80×10^4 MW-s, which corresponds to 3.80×10^7 kJ. The free energy provided by the hydrogen-oxygen fuel cell is given by

$$\mathrm{H_2} + 1/2\,\mathrm{O_2} \rightarrow \mathrm{H_2O}\,(gas),\ \ \Delta G = -229\,\mathrm{kJ/mol} \tag{39}$$

During the trip to Los Angeles, the tube vehicle will thus produce 1.66×10^5 moles of water, corresponding to a volume of 2.99×10^3 L of liquid water at 298 K. Because the tube vehicle stores the

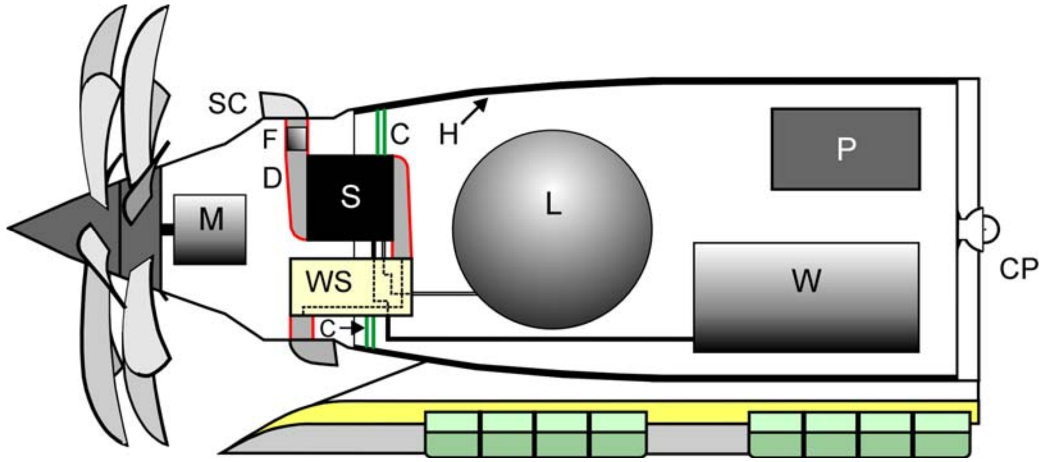

Fig. 9. Layout of locomotive. M = propulsion motor(s); SC = hydrogen scoop; F = axial fan; D = hydrogen duct system; S = fuel-cell stack; WS = water separator and LOX evaporator; W = water holding tank; H = liquid-to-hydrogen heat exchanger; C = coolant lines; L = LOX system, liquid oxygen plus hardware; P = power electronics; CP = genderless ball-and-socket coupling. As computed in the text, stack S is represented by a cube with sides 0.75 m, LOX system L is represented by a sphere of diameter 1.77 m, and the water holding tank W, a horizontal cylinder, has a volume of 1.49 x 10^3 L. Components S, L, and W are to scale, and each locomotive contains half of the total power and storage system. Hydrogen enters and exits the duct system D via opposite-facing scoops (SC), one at the top and one at the bottom; the scoops rotate 180^o when the vehicle reverses direction. WS separates water from cathodic oxygen and removes traces of water from the hydrogen exit stream via the LOX evaporator. Axial fan F is required when the vehicle operates at low speed or is stopped.

product water onboard, unlike conventional vehicles, it gains weight as it operates. From Equation (39), the corresponding number of moles of diatomic oxygen is 8.30 x 10^4 mol, which corresponds to a mass of 2.66 x 10^3 kg. With a density of 1.14 kg/L at its boiling point of 90 K [29], the total volume of LOX is 2.33 x 10^3 L, or 2.33 m^3.

Each of the two locomotives will store half of the total water and LOX for the trip from New York City to Los Angeles. Thus, the volume of stored water in each will be 1.49 m^3 and the volume of stored LOX will be 1.16 m^3. Our study of another vehicular cryogenic liquid (hydrogen) found a storage efficiency of only 0.37 [30]; that is, only 37% of the total volume of the storage system was the liquid, and the remainder was the tank, vacuum insulation, expansion volume, piping, valves, and similar storage infrastructure. If we assume a storage efficiency of 0.40 for LOX, we require a LOX system volume of 2.91 m^3 on each locomotive to store the required 1.16 m^3 for the trip. As a schematic, this volume corresponds to a sphere having a diameter of 1.77 m.

How much hydrogen is required to fill the tube from New York City to Los Angeles? Using the hydrogen density of Table 1, calculation shows that the mass of hydrogen is 1.03 t/km, or 4,080 t total. Since the worldwide annual production of hydrogen is 45 million t [31], this amount of hydrogen is less than 0.01% of annual production.

Using the volumes computed above for stacks, LOX, and water, Figure 9 is a schematic of the component layout of either of the two locomotives in a train. Only half of the total power and storage system is packaged in each of the two locomotives. The result, based on the aerodynamic calculations above, shows that the concept of a hydrogen tube vehicle is technically feasible: it is possible to package these critical components, along with other components, in a 2.69 outside diameter vehicle that runs in a 4.00-m inside diameter tube, and the vehicle can travel from New York City to Los Angeles at a speed of 1,500 km/h.

The biggest technical challenge is the gas bearings, in particular, maintaining adequate bearing clearance and dimensional stability of such a large system in the face of potential ground movement. That air bearings are capable of supporting a load comparable to the tube vehicle, while operating on a relatively crude surface, is demonstrated by the Airfloat compliant-seal system (see Fig. 6). Moreover, the feasibility of externally pressurized air bearings for rocket sleds has been analyzed and found to be feasible for levitation at Mach 6 [21]; only because of increased aerodynamic drag and weight were they rejected in place of self-acting air bearings. The weight penalty was as little as 230 kg, which is a small penalty for most transport vehicles, but it is impractical for a rocket sled that must accelerate from rest to Mach 6 in a few seconds.

Although I believe externally pressurized hydrogen gas bearings are potentially more efficient and less costly than magnetic levitation, if the gas-bearing concept presented here proves impractical, magnetic levitation (EMS) is an alternative that will work [6].

Another critical issue affecting feasibility is safety from fire or detonation within the tube. The flammability limits of hydrogen in air are 4-74% (v/v) [4]. Thus, there is no possibility of flammability or detonation within the tube until the air concentration inside reaches the <u>upper</u> flammability limit of hydrogen, that is, until air leaks into the tube in such quantity as to reduce the hydrogen concentration from 100% to 74%. Because the tube is closed at both ends and its hydrogen pressure is slightly above 1 bar, there will be no in-rush of air in the event of a tube rupture. If the tube were to rupture, and a source of ignition were present, there would initially be a flame <u>outside</u> of the tube as hydrogen exited and entered the surrounding air. Once the pressure in the tube fell to that of the outside air, entrance of the flame into the tube would be limited by the rate of air diffusion into the tube. Although the rate of air diffusion would depend on the size of the breach, it would likely be a slow process, and the flame would spontaneously extinguish as it progressed farther down the tube. According to this scenario, detonation within the tube seems unlikely. The scenario suggests that fire safety (as well as aerodynamic performance of the vehicle) will be enhanced by operating the tube at a hydrogen pressure minimally above ambient pressure.

The fire and detonation hazard should be similar to that of natural-gas pipelines, which operate worldwide and within urban areas, including gas pipes to homes. For example, the Trans-Canada pipeline is a 3,700-km, 0.91-m diameter natural-gas pipeline [10]. While gas pipelines occasionally are breached and the gas burns (for example, following a natural-gas explosion within a home), the consequence is not fire or detonation throughout the pipeline network. The risk for the hydrogen tube is thus expected to be manageable and acceptable.

Combustion inside the vehicle would be a possible hazard if the lower flammability limit were reached during a leak into the vehicle, i.e., if the vehicle itself were breached. Suffocation of passengers is also a hazard if hydrogen leaked into the vehicle, but the risk would be comparable to suffocation due to depressurization in high-altitude commercial aircraft. If ground movement, as in an earthquake, resulted in vee-way deformation, the vehicle could drag or crash on the vee-way – this would severely damage the vee-way or bearing pads, but it would not necessarily be a significant safety hazard to passengers, certainly less of a hazard than an airplane crash. Tube placement should allow ground movement with minimal deformation of the vee-way. Earthquake-resistant buildings are well studied, and one approach is to have the structure passively sit on top of the ground, like a box sitting upon a surface, rather than be anchored within the ground. That a large pipeline can successfully operate in an area of known tectonic faults is demonstrated by the Los Angeles Aqueduct, consisting in part of 8-12 ft steel pipe, which has been in operation since 1913 [8]. A tube passenger car will require an onboard oxygen supply for passengers and carbon dioxide scrubbing of the car's air.

4. Open Issues

The following unresolved issues should be addressed through engineering analysis, engineering design, and experimental work such as hydrogen wind-tunnel tests:

- Determine the optimum difference between the outside diameter of the vehicle and the inside diameter of the tube. A large gap will decrease vehicle drag but will increase infrastructure costs. Measure the effect on vehicle drag (primarily viscous drag with the tube inner surface) of operation within an enclosed tube rather than a free hydrogen atmosphere. Tube viscous drag will be a decreasing function of the vehicle-tube gap and the smoothness of the tube's inner surface.

- Design and test a prototype of the active levitation system. By sensing vee-way geometry ahead of the vehicle, the system would dynamically vary bearing-pad geometry to conform to curvature and twisting of the vee-way in normal operation and to accommodate deformation by ground movement. Determine the optimum included angle of the vee-way and the optimum bearing gap h that simultaneously minimizes levitation power, maximizes resistance to vee-way deformation, and maximizes vehicle dynamic stability. Airfoils may enhance stability.

- Undertake detailed infrastructure engineering design, including layout of the overall tube system, hydrogen makeup apparatus, hydrogen purification subsystem, airlocks to allow rescue of a disabled vehicle, and tube structural support and placement to minimize deformation due to ground movement.

- Conduct formal safety analyses of the tube's fire and detonation scenarios, as discussed above, and accordingly design hydrogen sensors and fire suppression devices. Undertake engineering design of onboard safety and support systems such as hydrogen sensors, fires suppression equipment, passenger oxygen supply, and carbon dioxide scrubbers.

- Estimate capital and recurring costs of the system. Capital costs include cost of the tube; laying of the tube, including structural support to obviate ground movement; the initial hydrogen atmosphere; the vehicle itself; and tube support infrastructure (hydrogen makeup apparatus, hydrogen purification subsystem, and vehicle-recovery airlocks). Operating costs, in cost per kg-km of payload, include hydrogen fuel, labor, operation of the tube infrastructure, and maintenance costs such as tube maintenance and occasional or gradual replacement of the hydrogen atmosphere.

5. Conclusions

The central concept of this paper is that operation of a vehicle in a hydrogen atmosphere would move the transonic region to much higher values and drag would be reduced relative to air. A hydrogen atmosphere requires that the vehicle operate in a hydrogen-filled tube or pipeline. The proposed vehicle runs on a guideway, is propelled by propfans, and flies on a hydrogen aerostatic fluid film. Vehicle power is provided by onboard hydrogen-oxygen fuel cells. Hydrogen fuel is taken from the tube itself, liquid oxygen (LOX) is carried onboard, and the product water is collected and stored until the end of a run. The system solves the open problem of onboard vehicular hydrogen storage.

Feasibility is shown by comparing the hydrogen tube vehicle with a mid-sized turboprop airliner, the Bombardier Dash 8 Q400. Based on aerodynamic analysis of the Q400, the tube vehicle will require 2.0 MW of net power to run at 1,500 km/h, which is supersonic with respect to air. It requires 2.64 h to travel from New York City to Los Angeles, consuming 2,330 L of onboard LOX during the trip. Part of the feasibility analysis shows that it is possible to package the fuel-cell stack, LOX system, and water holding tank, along with other components, within each locomotive. Compared to the Q400, the supersonic tube vehicle would be approximately twice as fast, require one-third the power, and consume one-tenth the energy to make the transcontinental trip.

I propose that the hydrogen tube vehicle has the potential to displace jet airplanes for high-speed transport: It would be faster, more energy efficient, and operate independent of the weather. Principal challenges facing the system are: (1) high absolute infrastructure cost, (2) maintenance of adequate hydrogen gaps in the aerostatic levitation and guidance system, and (3) possibly dynamic instability of the levitated vehicle.

References

[1] Anderson DF, Eberhardt S. Understanding flight. New York: McGraw-Hill, 2001.
[2] Kermode AC (rev. Barnard RH, Philpott DR). Mechanics of flight. 11th ed, Harlow, England: Pearson-Prentice Hall, 2006.
[3] Minto DW. CTEIP Funded advances in hypersonic testing at the Holloman High Speed Test Track. In: Proceedings of the 24th AIAA Aerodynamic Measurement Technology and Ground Testing Conference, American Institute of Aeronautics and Astronautics publication #2004-2740, Portland, Oregon, USA, 28 June – I July 2004.
[4] Lide DR, editor-in-chief. CRC Handbook of chemistry and physics, 88th ed. Boca Raton, FL, 2008.
[5] Haut RC, Adcock JB. Cryogenic hydrogen as a wind tunnel test gas. J. Aircraft 1977; 14(12): 1155-1156.
[6] Final report on the National Maglev Initiative. National Transportation Library, US Department of Transportation, Washington, DC, last updated 6 December 2004.
[7] SPG Media Limited, 2007. Website: http://www.water-technology.net/projects/gmr/.
[8] Di Pol J. The black pipes. Historical Society of the Upper Mojave Desert, May 2006, 21(5). Website: http://www.maturango.org/May06.html.
[9] Vincent-Genod J. Fundamentals of pipeline engineering. Houston, TX: Gulf Publishing Company, 1984.
[10] Liu H. Pipeline engineering. Boca Raton, Florida: CRC Press, 2003.
[11] Shevell RS. Fundamentals of flight, 2nd ed. Englewood Cliffs, NJ: Prentice Hall, 1989.
[12] Schimming P. Counter rotating fans: an aircraft propulsion for the future?. J. Thermal Science 2003;12(2):97-103.
[13] Houghton EL, Carpenter PW. Aerodynamics for engineering students. 5th ed, Burlington, MA: Butterworth-Heinemann, 2003.
[14] Neely M. "Antonov An-70," 2007. Website: http://www.theaviationzone.com.
[15] Jackson P, editor-in-chief. Jane's All The World's Aircraft. Alexandria, VA, 2004.
[16] Bombardier Aerospace, Toronto, Canada, 2006. Website: http://www.q400.com/q400/en/description.jsp.
[17] Larminie J, Dicks A. Fuel cell systems explained. Chichester, England: John Wiley, 2000.
[18] Gross WA, Matsch LA, Castelli V, Eshel A, Vohr JH, Wildmann M. Fluid film lubrication. New York: John Wiley & Sons, 1980.
[19] Devitt D. Air bearings eliminate static friction and stick-slip that compromise precision. Machine Design Magazine, 2004.

[20] Szeri AZ. Fluid film lubrication. Cambridge, UK: Cambridge University Press, 1998.
[21] Meier RC, Smith AF. Feasibility study of air bearing rocket sled slippers. Air Force Missile Development Center Technical Report, Holloman Air Force Base, New Mexico, 1966.
[22] Airfloat, LLC, 2007. Website: http://www.airfloat.com.
[23] Abbott T. Airfloat, LLC, personal communication, 31 July 2007.
[24] Slocum A, Basaran M, Cortesi R, Hart AJ. Linear motion carriage with aerostatic bearings preloaded by inclined iron core linear electric motor, Precision Engineering 2003, 27: 382-394.
[25] Gibbs P, Geim A. Is magnetic levitation possible? 18 March 1997. Website: http://www.weburbia.com/physics/levitation.html.
[26] Smith HC, The Illustrated Guide to Aerodynamics, 2nd ed. Blue Ridge Summit, PA: TAB books, 1992.
[27] Hirst E. Energy-intensiveness of transportation. J. Transportation Engineering Division 1973, American Society of Civil Engineers; 99(1):111-122.
[28] Miller AR, Hess KS, Barnes DL, Erickson, TL. System design of a large fuel cell hybrid locomotive. J. Power Sources 2007; in press.
[29] The Merck Index, 13th ed., Whitehouse Station, NJ: Merck & Company, 2001.
[30] Miller AR, Hess KS, Barnes DL. Comparison of practical hydrogen-storage volumetric densities. Proceeding of the National Hydrogen Association Annual Hydrogen Conference, San Antonio, 21 March 2007.
[31] BMW World, 2005. Website: http://www.bmwworld.com/hydrogen/faq.htm.

APPENDIX A

Working Model Demonstrating Levitation and Propulsion

Following submission of this paper, we have completed a working model that demonstrates two essential features of the proposed supersonic tube vehicle: levitation on a gas film and concurrent propulsion by a propeller. A photograph of the model is shown in Fig. A1.

The vehicle operates in air on a one-meter long aluminum 135^o vee-way and four 4 x 40 x 65 mm bearing pads. Rather than taking power from a fuel cell, it uses an onboard battery to operate the electrically powered 130-mm diameter single-rotating propeller. Gas, either nitrogen or hydrogen, for the gas-bearing levitation system is provided from an off-board compressed-gas tank, which is connected to the operating vehicle by a flexible silicone tube. The levitation system uses a passive suspension system that assures conformation of the bearing pads to the vee-way, even in the face of bowing or twisting of the vee-way.

This working model, besides demonstrating the essential feasibility of the concept vehicle, corrects one error in the literature: A feasibility study [21] concerning use of aerostatic gas bearings in hypersonic rocket sleds states that such a vehicle cannot be self-lifting because when the bearing gap h = 0 there will be no gas flow and hence no lift. However, in contrast, the working model is self-lifting and shows that the assertion of no self-lifting, while correct in theory, is not correct in practice. The vehicle is self-lifting because the mating of bearing pads and vee-way is not perfect and therefore h is not equal to zero in practice.

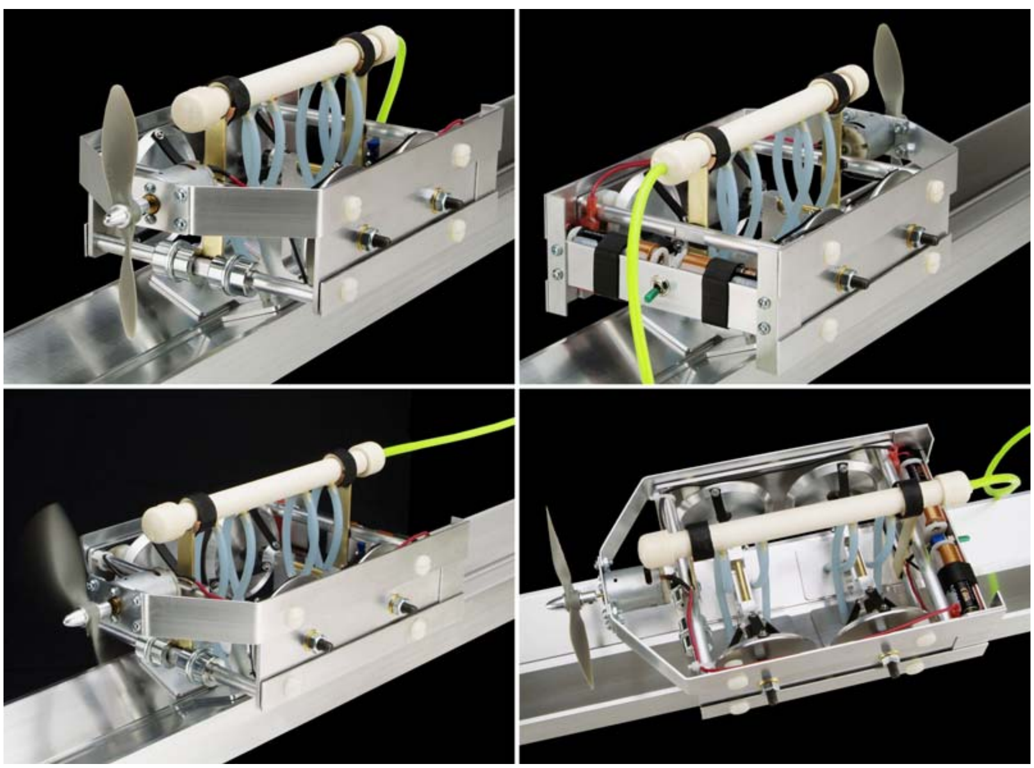

Fig. A1 - Working model demonstrating gas-film levitation and propulsion. Clockwise from top-left: (1) Three-quarter front view showing propulsion motor and propeller. For scale, propeller diameter is 130 mm. The white tube at the top of the vehicle is the gas manifold. (2) Three-quarter rear view showing the four-AA battery module and on/off switch. Compressed nitrogen is provided to the vehicle via the green silicone tube. (3) Top view showing blue silicone tubes feeding the gas bearing pads and suspension system that assures conformation of the pads to the vee-way. (4) Photograph of levitation and propulsion in action.